



Behavior of full-scale self-consolidating concrete beams in shear

A.A.A. Hassan, K.M.A. Hossain *, M. Lachemi

Department of Civil Engineering, Ryerson University, 350 Victoria Street, Toronto, ON, Canada M5B 2K3

ARTICLE INFO

Article history:

Received 16 May 2007

Received in revised form 20 March 2008

Accepted 25 March 2008

Available online 7 April 2008

Keywords:

Self-consolidating concrete

Shear resistance

Aggregate interlock

Dowel action

Design equations

ABSTRACT

An experimental investigation was conducted to study the shear strength and cracking behavior of full-scale beams made with self-consolidating concrete (SCC) as well as normal concrete (NC). A total of 20 flexurally reinforced concrete beams, with no shear reinforcement, were tested under mid-span concentrated load until shear failure occurred. The experimental test parameters included concrete type/coarse aggregate content, beam depth and the longitudinal reinforcing steel ratio. The beam depth ranged from 150 to 750 mm while the shear span-to-depth ratio (a/d) was kept constant in all beams. The two longitudinal reinforcing steel ratios used were 1% and 2%. The performance of SCC/NC beams was evaluated based on the results of crack pattern, crack widths, loads at the first flexure/diagonal cracking, ultimate shear resistance, and failure modes. The ultimate shear strength of SCC beams was found to be slightly lower than that of NC beams and the difference was more pronounced with the reduction of longitudinal steel reinforcement and with the increase of beam depth. The performance of code based equations in predicting the shear resistance of SCC/NC beams is also presented. The recommendations of this paper can be of special interest to designers considering the use of SCC in structural applications.

© 2008 Elsevier Ltd. All rights reserved.

1. Introduction

Self consolidating concrete (SCC), one of the latest innovations in concrete technology, is a highly flowable high performance concrete that spreads readily under its own weight without the use of vibrators and achieves good consolidation without segregation even in a very congested structural member with large amount of steel reinforcement [1–6]. SCC also facilitates pouring concrete in higher free falls – concrete free fall of more than 3 m in depth was accomplished without segregation during the construction of the Akashi–Kaikyo suspension bridge in Japan in 1998 [1].

The lack of information regarding in situ properties and structural performance of SCC members is still a hindrance for this material to be used confidently by designers/engineers in practical applications [6,7]. In particular, there are some concerns among designers/engineers that SCC may not be strong enough in resisting shear because of the presence of comparatively smaller amount of coarse aggregates compared to normal concrete (NC) which can lead to the formation of smooth fractured surfaces and subsequent development of weak aggregate interlock mechanism [8].

Taylor [9] investigated reinforced normal concrete beams without shear reinforcement, and reported that the shear strength is derived from the contributions of compression shear zone (ranging between 20% and 40%), aggregate interlock mechanism (ranging

between 35% and 50%), and the dowel action of longitudinal reinforcement (ranging between 15% and 25%). Hence, a major component of the shear transfer in the fractured interface arises from the friction forces that develop across the diagonal shear cracks due to “aggregate interlock” which provides resistance against slip. The aggregate interlock is greatly influenced by the beam size – as the depth of the beam increases, the crack widths at points above the main longitudinal reinforcement tend to increase. This leads to a reduction in aggregate interlock across the crack, resulting in the reduction of shear stress [10–13]. Also, the aggregate interlock is influenced by the longitudinal reinforcement ratio and this component of shear strength is more significant if the cracks are narrow. Thus, higher percentage of longitudinal reinforcing steel which reduces the shear crack width would allow the concrete to resist more shear [14,15].

This paper presents the results of an investigation dealing with the overall shear behavior of 20 full-scale reinforced concrete beams, with no shear reinforcement, made with SCC and NC. It is important to study the shear failure mechanism of large-scale reinforced concrete beams without web reinforcement to better understand the failure mechanisms in beams with stirrups [16]. The test parameters include concrete type (SCC or NC)/coarse aggregate content, beam depth and the longitudinal reinforcing steel ratio. Shear strength, crack patterns and crack width of the experimental beams with SCC and NC are compared. The performance of code based design equations in predicting the shear resistance of SCC/NC beams is also presented.

* Corresponding author. Tel.: +1 416 979 5000x7867; fax: +1 416 979 5122.
E-mail address: ahossain@ryerson.ca (K.M.A. Hossain).

2. Experimental program

2.1. Details of beam specimens

Twenty reinforced concrete beams (10 made with SCC and 10 with NC), designed only for adequate flexural reinforcement and having no shear reinforcement were tested. Table 1 and Fig. 1 show the geometric dimensions of SCC/NC beams. All beams were 400 mm wide (b) with total depth (h) ranging from 150 to 750 mm. The shear span-to-total depth ratio (a/h) was kept constant at a value of 2.5 to ensure shear rather than bending failure of all beams [17–19] (Table 1 and Fig. 1). Two flexural reinforcement configurations were used for the beams with longitudinal reinforcement ratios (ρ_w) of 1% and 2%. Cross-sectional dimensions and reinforcement layouts of beams are shown in Fig. 2. The beams were designated by concrete type, total beam depth (h), and longitudinal reinforcement ratio (ρ_w). The beam designation included a combination of letters and numerics: SCC or NC to indicate the concrete type; 1 or 2 to indicate the longitudinal reinforcement ratio; and 150, 250, 363, 500 or 750 to designate the total height. For example, a SCC beam having 1% ρ_w with a total height of 750 mm is designated as 1SCC750 (Table 1).

2.2. Materials

Concrete mixes were designed to study the effect of lower coarse aggregate content in SCC (which is normal for SCC) compared with that in NC. A total of two mixes were used to cast experimental beams: one NC mixture with 1130 kg/m³ of coarse aggregate and one SCC mixture with 25% lower coarse aggregate content. The volume change in the mix design was compensated with an increase in sand content in SCC mixture. Such significant difference was intended to study the effect of aggregate interlock on the shear strength reduction, if any. Details of SCC/NC concrete mix proportions are presented in Table 2. The water-to-cementitious materials ratio was kept constant at 0.4 for both SCC and NC mixes in order to achieve similar compressive strength. Type GU Canadian cement similar to ASTM Type I and slag cement were used as cementitious materials for both SCC and NC. Natural sand and 10 mm maximum size stone were used as fine and coarse aggregates, respectively. High range water reducer (HRWR) similar to Type F of ASTM C 494 [20] and water reducer (WR) similar to Type A of ASTM C 494 [20] were used to adjust the flowability and cohesiveness of SCC and NC mixtures, respectively.

Table 1
Details of experimental beams

Beam designation	Total length (L ; mm)	Effective span (S ; mm)	Total depth (h ; mm)	Effective depth (d ; mm)	Longitudinal steel ratio ($\rho_w = 100A_s/bd$; %)
1SCC150	1050	750	150	102.5	1
1NC150				100.0	2
2SCC150					
2NC150					
1SCC250	1750	1250	250	202.5	1
1NC250				197.5	2
2SCC250					
2NC250					
1SCC363	2340	1815	363	310.5	1
1NC363				305.5	2
2SCC363					
2NC363					
1SCC500	2500	3200	500	447.5	1
1NC500				442.5	2
2SCC500					
2NC500					
1SCC750	4500	3750	750	667.5	1
1NC750				650.5	2
2SCC750					
2NC750					

A_s , area of longitudinal steel; b , width of the beam = 400 mm; a , shear span = $S/2$.

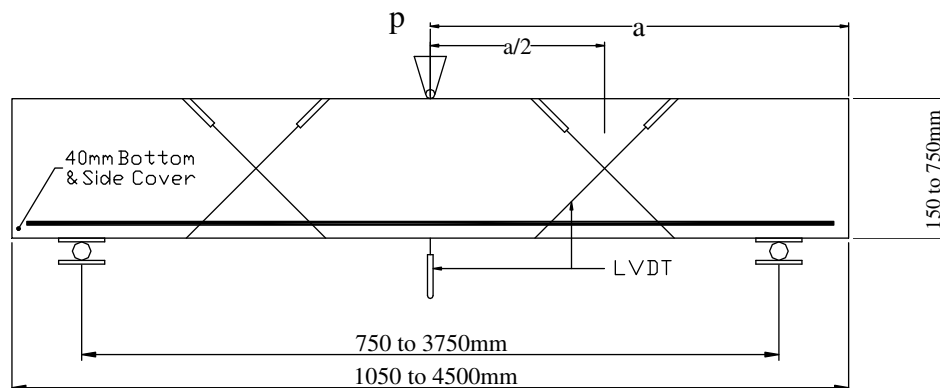


Fig. 1. Schematic diagram of experimental beam specimens.

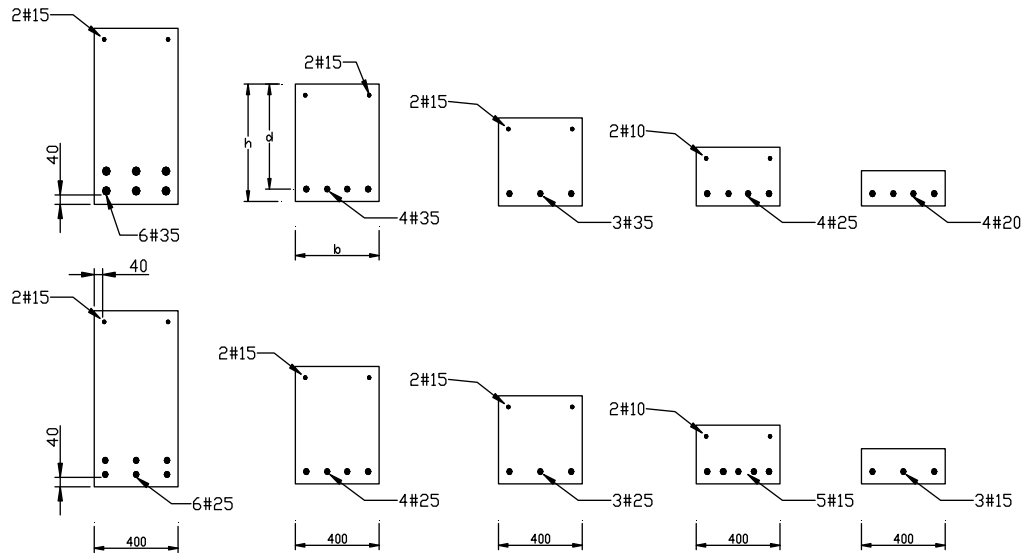


Fig. 2. Cross sections and reinforcement layout of beams with 1% and 2% ρ_w (dimensions in mm).

Table 2
Mixture proportions for SCC and NC mixtures

Concrete type	Type 10 cement (kg/m ³)	Slag cement (kg/m ³)	10 mm coarse aggregate (kg/m ³)	Fine aggregate (kg/m ³)	Water (kg/m ³)	HRWR ml/100 kg of binder	WR ml/100 kg of binder
SCC	315	135	900	930	180	850	0
NC	300	100	1130	725	160	0	300

Table 3 presents the fresh and strength properties NC and SCC mixtures. The traditional slump test according to ASTM C 143 [21] was conducted for NC. The slump flow test [22] was conducted to evaluate the viscosity and flowability of SCC mixture while V-funnel [23] and L-box [24] tests were conducted to evaluate the stability and the passing ability, respectively. Slump flow, flow time and L-box index values (Table 3) satisfied recommended values needed for a SCC. 100 × 200 mm control cylinders were used to determine the compressive (f_c) and the indirect tensile (f_{ct}) strength as per ASTM C 39 [25] and ASTM C 496 [26], respectively, for both NC and SCC mixtures.

The diameters of deformed bars used for reinforcing beams were 10, 15, 20, 25, and 35 mm (designated as “# bar dia” in Fig. 2). The deformed bars had an average yield strength of 480 MPa and an average tensile strength of 725 MPa.

2.3. Casting of beam specimens

The two concrete mixtures used in this investigation were delivered to Ryerson University Structures laboratory in 6 m³ trucks by Dufferin Concrete Group, Toronto – Canada. The delivered SCC mixture was successfully used in Pearson International airport project in Toronto, Canada, in the year of 2000 [27]. Immediately after concrete delivery, tests on fresh properties of the con-

crete mixtures as well as casting of beams in prepared wooden forms were carried out. SCC beams were cast without consolidation – the concrete was poured in the formwork from one side until it flow and reached the other side. Visual observation showed that the SCC properly filled the forms with ease of movement around reinforcing bars in each reinforcement configuration. On the other hand, NC beams were consolidated using electrical vibrators and trowel finished for smooth top surfaces. The placement of NC beams was labor intensive and the time required to cast and finish each beam element was much longer than that required for SCC beams. Formworks were removed after 24 h of casting and the beams were moist cured for four days and then air cured until the date of testing.

2.4. Test setup, instrumentation and loading procedure

The beam specimens were tested as simply supported beams under three-point loading condition (Figs. 1 and 3). The test setup included the use of a hydraulic jack that applied load gradually on the mid-span of beam specimens until failure. Four linear variable displacement transducers (LVDTs) were attached at 45° on the front surface of each beam to measure the shear strain (Figs. 1 and 3). Another LVDT was placed directly under the mid-span of each beam to measure central deflection. In order to monitor the

Table 3
Fresh and hardened properties of SCC and NC mixtures

Concrete type	Slump (mm)	Slump flow		V-funnel flow time (s)	L-box			28-d f_c (MPa)	28-d f_{ct} (MPa)
		Flow (mm)	T500 (s)		Index (%)	T200 (s)	T400 (s)		
SCC	–	700	30	5.5	90	1.5	2	45	3.8
NC	80	–	–	–	–	–	–	47	4

T500, flow time to achieve 500 mm slump flow; T200 and T400, times taken by concrete to travel a horizontal distance of 200 and 400 mm, respectively.



Fig. 3. Test setup, instrumentation and testing and failure mode of a beam specimen.

development of strain in the longitudinal steel reinforcement with progressive loading, two electrical strain gauges were installed to the lower layer of the reinforcement directly under the loading point at mid-span. A computer aided data acquisition system automatically monitored load, displacements and strains at pre-selected time intervals throughout the loading history. The tests also provided information on the overall behavior of beams including development of cracks, crack patterns, crack width, load transfer mechanisms and failure modes. The load was applied in a load control fashion in three stages. The first and second stages correspond to 50% and 75% of the expected failure load, respectively, while the third stage corresponds to the failure load.

3. Test results and discussion

3.1. General cracking and failure behavior of SCC and NC beams

Fig. 3 shows a typical shear failure of an experimental beam. The cracks were outlined with a black felt tip marker and the crack width was determined and labeled at each loading stage (Fig. 3).

Fig. 4 shows crack patterns of SCC and NC beams at failure. During early stages of loading, fine vertical flexural cracks appeared around the mid-span of all beams, as expected. With the increase in load, new flexural cracks were formed away from the mid-span area. With further increase in load, those flexural cracks started to propagate diagonally towards the loading point and other new diagonal cracks began to form separately in locations farther away from the mid-span along the beam (Figs. 3 and 4).

In general, large size SCC/NC beams had more cracks and developed higher diagonal crack widths at failure irrespective of reinforcement ratio (1% or 2%). In most cases, shear failure of beams occurred shortly after a dominant diagonal shear crack (within one shear span or zone) extended to the top fibre as indicated in Figs. 3 and 4. In addition, failure of larger size beams was sudden compared to small size beams.

For both SCC and NC beams, the cracks extended up to 50% and 70% of the beam height at around 50% and 75% of the failure load, respectively. The angle for the early diagonal dominant shear

cracks was around 55° (to the beam longitudinal axis) while that for the failure diagonal cracks was around 35°. Since the shear span-to-total height ratio (a/d) was kept constant for all beams, the number of cracks before failure tends to increase with the height of the beam (5–6 in shallow and 11–12 in deeper beams).

3.2. Cracking load and crack width characteristics of SCC/NC beams

The first flexural cracking load was visually observed and then compared with values associated with change in slope of the load-deflection and load-longitudinal steel strain curves obtained from the test. The formation of first diagonal crack was also observed visually during the loading and was also verified most of the time by sudden jump in the elongation for any of the four diagonal LVDTs mounted on the surface of the beam (Figs. 1 and 3). Table 4 presents the loads at first flexure/shear crack, crack characteristics number of cracks, crack height and the failure crack width) and failure loads of all SCC/NC beams.

From Table 4, no significant difference was observed between SCC and NC beams with respect to the first flexural crack load, as expected. The ratio of the first flexural crack load to the failure load increases with the increase of beam depth in SCC/NC beams having 1% or 2% steel reinforcement (Table 4). First flexural crack load for SCC beams varied from 21% to 38% of the failure load (from shallow to deeper beams) compared with 20% to 33% of NC beams.

The first diagonal dominant shear cracks were developed around 32% of the failure load for shallow beams compared to 60% of deep beams (Table 4). The failure crack widths varied from 1 to 3 mm in shallow beams while crack width of up to 27 mm was observed in deeper beams (Fig. 4 and Table 4). In general, SCC beams exhibited slightly less number of cracks than NC beams. The number of diagonal shear cracks was also lower in SCC beams compared to NC beams. Otherwise, no significant difference was noted between SCC and NC beams in terms of crack widths, crack heights, crack angles or overall failure mode (Fig. 4 and Table 4).

From Table 4, it can be seen that the percentage ratio of the first diagonal crack load to the failure load in SCC beams increases from 34% to 65% with the increase of beam depth from 150 mm (shallow

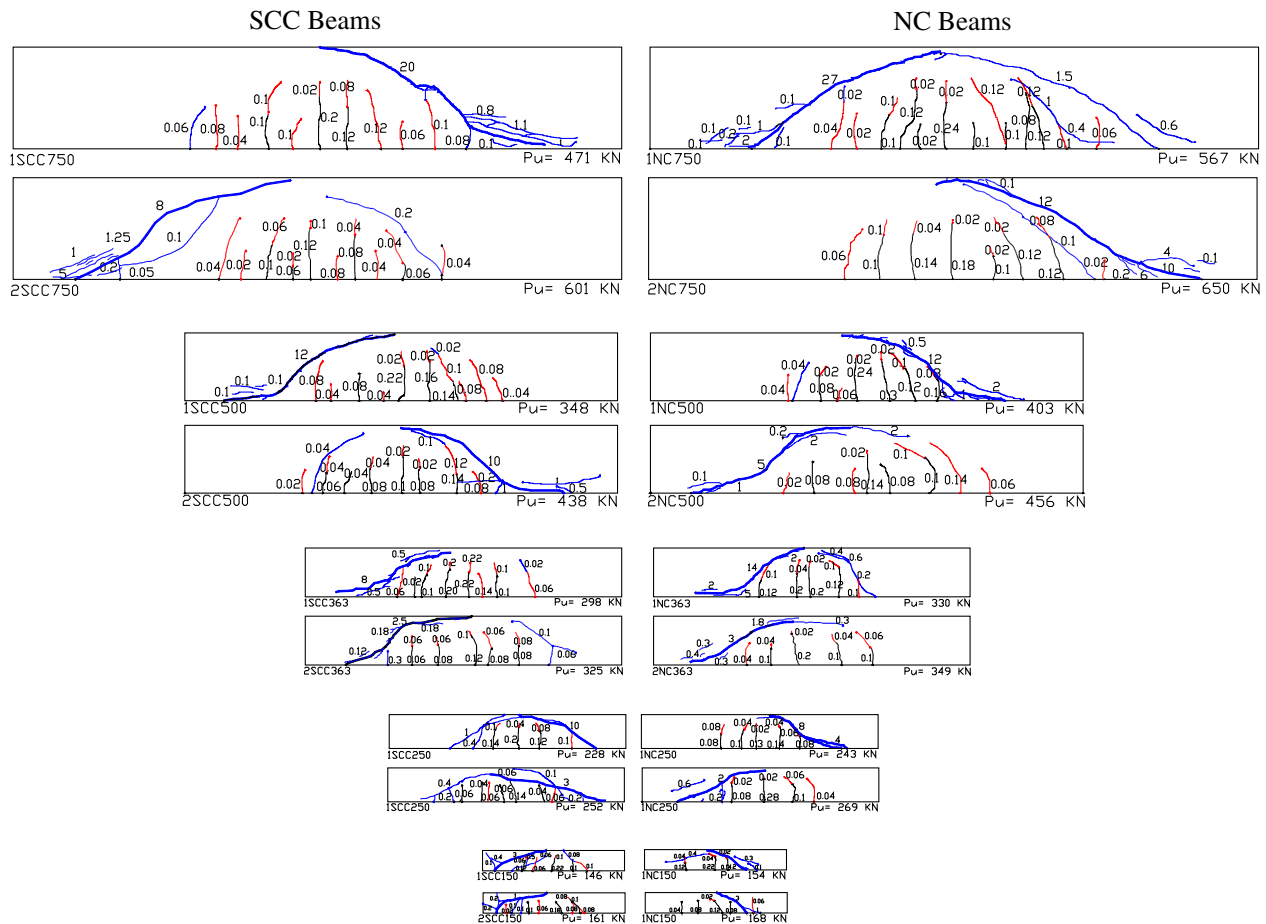


Fig. 4. Crack patterns of SCC and NC beams at failure (crack width in mm).

Table 4
Cracking loads and crack characteristics of experimental SCC/NC beams

Beam designation	Total applied load (P; kN)			Ratio (%)		Number of crack at failure	Maximum crack height (mm)	Maximum crack width at failure (mm)
	At first flexural crack (P_f)	At first diagonal crack (P_d)	At failure (P_u)	$100P_f/P_u$	$100P_d/P_u$			
1SCC150	32	49	146	22	34	6	116	3
1NC150	32	50	154	21	32	5	119	2
2SCC150	33	53	161	21	33	6	116	1
2NC150	33	50	168	20	30	6	114	3
1SCC250	58	74	228	25	32	6	189	10
1NC250	60	82	243	25	34	5	182	8
2SCC250	60	83	252	24	33	7	182	3
2NC250	54	85	269	20	32	6	184	2
1SCC363	90	141	298	30	47	8	251	8
1NC363	90	135	330	27	41	6	270	14
2SCC363	96	146	325	30	45	7	248	2.5
2NC363	94	132	349	27	38	5	251	3
1SCC500	109	200	348	31	57	10	362	12
1NC500	120	190	403	30	47	8	358	12
2SCC500	120	240	438	27	55	9	352	10
2NC500	135	205	456	30	45	8	356	5
1SCC750	180	320	471	38	68	11	495	20
1NC750	188	325	567	33	57	12	518	27
2SCC750	222	390	601	37	65	12	435	8
2NC750	205	350	650	32	54	9	446	12

beam) to 750 mm (deep beam) compared with 32–54% of corresponding NC beams. This indicates that SCC beams had lower post-diagonal cracking shear resistance capacity (derived from aggregate interlock plus dowel action) compared to NC beams.

Generally SCC/NC beams with lower steel ratio (1%) developed wider crack widths during loading stages and at failure compared to those with higher steel ratio (2%). This was expected as the presence of higher longitudinal steel ratio increases the resistance for

the cracks to open wider and to extend vertically. The average height of cracks before failure was more in beams with 1% reinforcement steel ratio (71% of the beam height) compared to beams with 2% reinforcement steel ratio (63% of the beam height). In general, cracks extended vertically up to the theoretically calculated neutral axis for each cracked SCC/NC beams (with both 1% and 2% steel reinforcement) with a maximum difference of 10%.

3.3. Shear resistance characteristics of SCC/NC beams

To analyze and compare the shear strength of beams, the ultimate shear load (V_u) is normalized to account for the difference in compressive strength between SCC and NC. Since the shear strength is proportional to the square root of the compressive strength of concrete (f'_c), the normalized shear load (V_{nz}) was calculated as follows:

$$V_{nz} = \frac{V_u}{\sqrt{f'_c}} \quad (1)$$

The normalized shear stress (v_{nz}) is then calculated as:

$$v_{nz} = \frac{V_{nz}}{bd} \quad (2)$$

Normalized shear load and stress for all experimental SCC/NC beams are tabulated in Table 5.

3.3.1. Influence of concrete type, beam depth and longitudinal steel ratio on normalized shear load (V_{nz})

While shear span-to-total depth ratio (a/h) of all beams were kept constant, the shear resistance of beams was found to depend on type of concrete, beam depth and longitudinal steel ratio. Figs. 5 and 6 show the variation of normalized shear load (V_{nz}) and normalized ultimate shear stress (v_{nz}), respectively, of SCC/NC beams having varying depths and longitudinal steel ratios. In general, SCC beams exhibited lower V_{nz} compared to NC beams for all beam depths (ranging from 150 to 750 mm) and for both longitudinal steel ratios (1% and 2%; Fig. 5). V_{nz} also increased with the increase of beam depth and longitudinal steel ratios, for both NC and SCC.

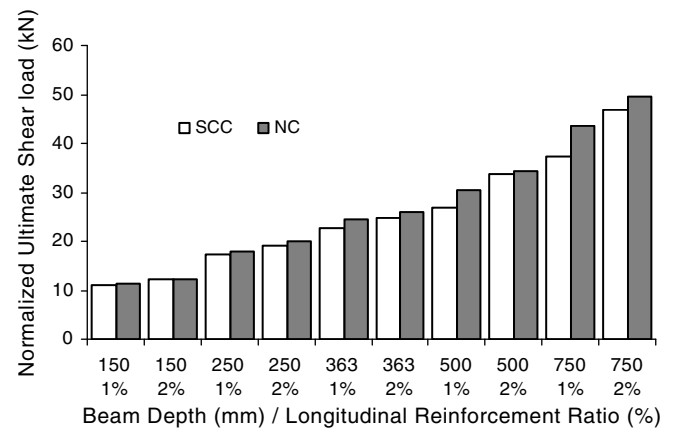


Fig. 5. Normalized ultimate shear load (V_{nz}) for SCC and NC beams.

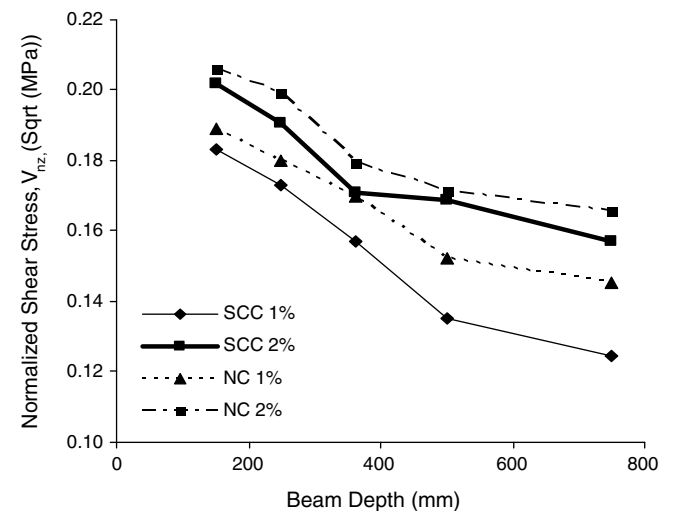


Fig. 6. Effect of beam depth on normalized shear stress (v_{nz}) for both SCC and NC beams.

Table 5

Shear resistance of SCC/NC beams from experiments and code based predictions

Beam designation	Experimental			Code based prediction		Comparison (Ratio)	
	Ultimate shear load (V_u ; kN)	Normalized ultimate shear load (Eq. (1); V_{nz})	Normalized ultimate shear stress (Eq. (2); v_{nz})	Ultimate shear load ACI (Eq. (3); kN)	Ultimate shear load CSA (Eq. (4); kN)	Ultimate shear (ACI/Exp.)	Ultimate shear (CSA/Exp.)
1SCC150	74	11.0	0.18	46	42	0.63	0.57
1NC150	78	11.3	0.19	46	42	0.59	0.54
2SCC150	81	12.1	0.20	47	47	0.58	0.58
2NC150	85	12.4	0.21	47	47	0.56	0.56
1SCC250	116	17.3	0.17	92	78	0.80	0.67
1NC250	123	18.0	0.18	92	78	0.75	0.63
2SCC250	128	19.1	0.19	96	89	0.75	0.70
2NC250	136	19.9	0.20	96	89	0.70	0.65
1SCC363	153	22.8	0.16	142	112	0.93	0.73
1NC363	169	24.6	0.17	142	112	0.84	0.66
2SCC363	166	24.8	0.17	150	130	0.90	0.78
2NC363	178	26.0	0.18	150	130	0.84	0.73
1SCC500	181	27.0	0.14	206	147	1.14	0.81
1NC500	209	30.4	0.15	206	147	0.99	0.71
2SCC500	226	33.7	0.17	219	172	0.97	0.76
2NC500	235	34.3	0.17	219	172	0.93	0.73
1SCC750	250	37.3	0.12	307	195	1.23	0.78
1NC750	298	43.5	0.15	307	195	1.03	0.65
2SCC750	315	47.0	0.16	321	225	1.02	0.71
2NC750	340	49.6	0.17	321	225	0.95	0.66

Normalized ultimate shear stress (v_{nz}) decreased with the increase of beam depth for both SCC and NC beams (Fig. 6). When beam depth increased from 150 to 750 mm, the normalized shear stress of beams with 1% steel reinforcement decreased by 32% for SCC compared to 23% of NC. Similarly when beam depth increased from 150 to 750 mm, the normalized shear stress of beams with 2% steel reinforcement decreased by 22% for SCC compared to 20% of NC.

Higher shear resistance of NC beams compared to their SCC counterparts was observed in beams having larger depths and lower longitudinal steel reinforcement ratio (Figs. 5 and 6). The maximum difference in shear resistance was observed in 1NC750 beam which showed 17% higher V_{nz} compared to its SCC counterpart 1SCC750.

The portion of the shear transfer through aggregate interlock, which normally represent up to 50% of the total shear transfer, is greatly affected by the coarse aggregate content. In this study, NC contains 25% more coarse aggregate than SCC. Hence, the reduction in coarse aggregate content in SCC beams is believed to be the main reason for the lower ultimate shear resistance of SCC beams compared to NC beams.

Fig. 7 shows the variation of the percentage ratio r_L ($=100 \times V_{nz-NC}/V_{nz-SCC}$) of normalized ultimate shear load of NC beam (V_{nz-NC}) to that of SCC beam (V_{nz-SCC}) with beam depth and longitudinal steel ratio. In general, the r_L increased with the increase of beam depth and the rate of increase, was much higher for beams containing 1% longitudinal reinforcement compared to those with 2%. Beams containing 1% reinforcement showed higher r_L compared with those containing 2% reinforcement irrespective of beam depth. For an increase of steel ratio from 1% to 2%, the r_L was increased from 2% to 3% for 150 mm depth beams compared with corresponding 5% to 17% of 750 mm depth beams. This indicates that SCC beams have lower shear strength compared to NC beams and the lowering of strength increases with the increase of beam depth and with the decrease of reinforcement ratio. However, for shallow beams (for example, beam depth of 150 mm), the influence of type of concrete and reinforcement ratio on the shear strength seems to be negligible for the range of beams tested in this study.

The shear is transferred in a cracked beam through aggregate interlock in the cracked concrete, resistance of un-cracked concrete in compression zone and dowel action of the longitudinal steel. For beams having higher longitudinal steel reinforcement, the post-

cracking shear resistance through the dowel action and the un-cracked concrete in compression zone is higher compared to beams having lower longitudinal steel reinforcement. The portion of the shear transfer through aggregate interlock in post-cracking stage is less for beams with higher reinforcement ratio which is beneficial for SCC because of its weaker aggregate interlock mechanism due to the presence of lower coarse aggregate. This explains why beams containing 1% reinforcement showed higher r_L compared to those with 2%.

Higher shear resistance of NC beams compared to SCC beams with the increase of beam depth (as evident from the increase of r_L with the increase of beam depth in Fig. 7) can also be attributed to the development of longer and relatively wider cracks in deeper beams which means higher portion of post-cracking shear transfer through aggregate interlock is warranted compared to shallow beams [28]. As SCC generates lower shear resistance through aggregate interlock, overall shear resistance of a SCC beam decreases with the increase of beam depth compared to its NC counterpart.

4. Performance of code based shear prediction of SCC beams

The ultimate shear resistances of experimental SCC/NC beams without shear reinforcement are calculated based on code based equations. In this study, performance of ACI and CSA based design Eqs. (1) and (2), respectively, is studied.

As per ACI [29], the shear resistance (V_u) of beams without shear reinforcement at diagonal (inclined) cracking (where M_f occurs simultaneously with V_f at a section) can be obtained as (based on SI unit):

$$V_u = 0.158\sqrt{f_c}bd + 17.24\rho_w \frac{V_f d}{M_f} bd \leq 0.29\sqrt{f_c}bd \quad (3)$$

where V_f is the factored shear force at section; M_f is the factored moment at section; b is the beam width; d is the effective depth of beam cross-section; and A_s is the area of non-prestressed tension reinforcement in the beam.

As per CSA specification [30], shear resistance (V_u) for beams without shear reinforcement can be obtained as (based on SI unit):

$$V_u = \beta\sqrt{f_c}bd_v \quad (4)$$

The factor β can be calculated as:

$$\beta = \frac{520}{(1 + 1500\varepsilon_x)(1000 + S_{ze})} \quad \text{and} \quad S_{ze} = \frac{35S_z}{15 + a_g} \leq 0.85S_z \quad (5)$$

where d_v is effective shear depth which can be taken as the greater of $0.9d$ or $0.72h$; ε_x is the longitudinal strain at mid-depth of the member due to factored loads which can be derived as $\varepsilon_x = \frac{M_f/d_v + V_f}{2E_s A_s}$; E_s is the modulus of elasticity of non-prestressed reinforcement; S_z ($=d_v$) is the crack spacing parameter dependent on crack control characteristics of longitudinal reinforcement and a_g is the maximum size of aggregate in concrete.

Table 5 presents the ultimate shear load derived from experiments and code based predictions. Figs. 8 and 9 compare the performance of code based equations (ACI – Eq. (3) and CSA – Eq. (4)) in predicting the ultimate shear load (V_u) of SCC/NC beams having 1% and 2% ρ_w and no shear reinforcement. CSA (Eq. (4)) under predicted the ultimate shear strength of SCC/NC beams irrespective of beam depth (150–750 mm) and longitudinal reinforcement ratio (1% and 2%) as the ratio of experimental to CSA prediction ranges between 0.54 and 0.81 with a mean value of 0.68 (Table 5 and Figs. 8 and 9). In general, CSA is more conservative than ACI (its conservativeness increases with the increase of beam depth) and can be used safely for the prediction of ultimate shear resistance of both SCC and NC beams as confirmed from this study.

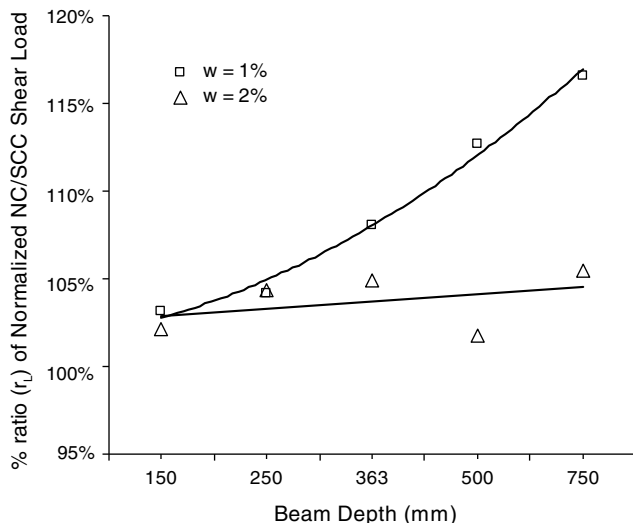


Fig. 7. Percentage ratio (r_L) of normalized ultimate shear loads ($r_L = 100 \times U_{nz-NC}/U_{nz-SCC}$).

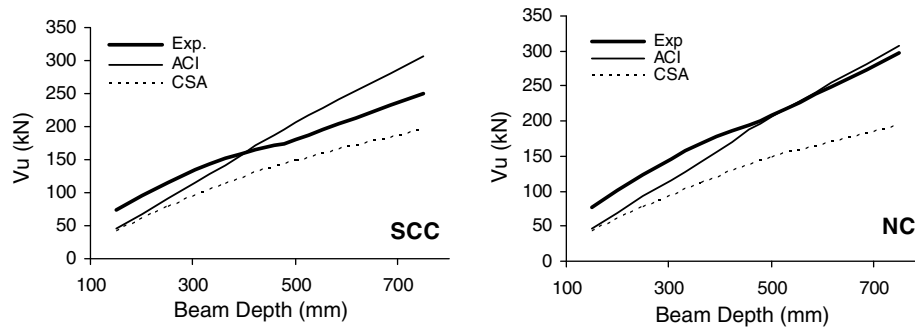


Fig. 8. Ultimate shear strength (V_u) – experiments and code predictions (beams with 1% ρ_w).

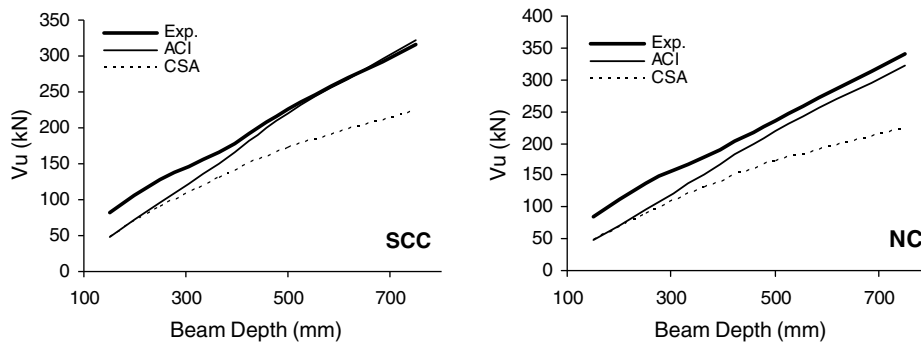


Fig. 9. Ultimate shear strength (V_u) – experiments and code predictions (beams with 2% ρ_w).

ACI equation is found to safely predict the ultimate shear strength of NC beams with 2% reinforcement (ratio ranges between 0.56 and 0.95). The ratio of ACI predicted to experimental values for NC beams with 1% reinforcement started with 0.59 for 150 mm beam depth and increased to 1.03 for the 750 mm beam depth. ACI equation may not be safe for NC beams with larger depth and low longitudinal reinforcement. The unconservative prediction of the ACI code for larger size members with low reinforcing ratios has also been recognized by other researchers [31].

The ratio ACI predicted to experimental values ranges between 0.63 (for 150 mm beam depth) and 1.23 (750 mm beam depth) for SCC beams with 1% reinforcement while between 0.58 (for 150 mm beam depth) and 1.02 (for 750 mm beam depth) for beams with 2% reinforcement. The ACI equation is found to be conservative for SCC beams up to a beam depth of 363 mm (for beams with 1% longitudinal reinforcement) and 500 mm (for beams with 2% longitudinal reinforcement) while it over predicts the shear strength of deeper beams.

5. Conclusions

The shear resistance of self-consolidating concrete (SCC) is described and compared with normal concrete (NC) based on test results of experimental beams having no shear reinforcement. The crack pattern, crack width, crack load, failure modes and overall shear resistance at failure are critically analyzed to study the influence of variable geometric, material and longitudinal reinforcement parameters. Based on the results presented in this paper, the following conclusions are warranted:

- Overall, SCC showed similar shear resistance characteristics in pre-cracking stage as compared with NC. No significant difference was noted between SCC and NC beams in terms of crack widths, crack heights, crack angles or overall failure mode. The ultimate shear load of SCC/NC beams increased with the

increase of longitudinal reinforcement while ultimate shear stress decreased with the increase of beam depth irrespective of either 1% or 2% longitudinal reinforcement ratios, as expected.

- SCC beams showed lower ultimate shear load compared to their NC counterparts and the shear strength reduction was higher in deeper beams with lower longitudinal steel ratios. When beam depth was increased from 150 to 750 mm, the shear stress of beams with 2% longitudinal reinforcement ratio dropped by 22% (SCC) and 20% (NC) compared to 32% (SCC) and 23% (NC) of beams with 1% reinforcement ratio. NC beam with 750 mm depth and 1% reinforcement ratio showed 17% higher ultimate shear load compared to its SCC counterparts. Lower shear strength of SCC is attributed to the development of lesser aggregate interlock as a consequence of the presence of lower quantity of coarse aggregate compared to NC.
- CSA based equation is found to be conservative in predicting the shear strength of both SCC/NC beams irrespective of beam depth or longitudinal reinforcement ratio and the predicted values were generally lower than the experimental values. Although the ACI equation for shear strength is conservative for NC beams with 2% reinforcement ratio irrespective of beam depth, it is not conservative for deeper NC beams with 1% reinforcement ratio as well as for deeper SCC beams with either 1% or 2% reinforcement ratio. Hence for deeper beams with comparatively lower longitudinal reinforcement, ACI equation may not be safe and particularly the risk of over prediction is higher for SCC beams compared to NC beams.

Acknowledgements

The authors gratefully acknowledge the financial assistance of the Natural Sciences and Engineering Research Council (NSERC) of Canada for this research project. Thanks to Mr. John Pontarollo and Mr. Dennis Baker of St. Lawrence Cement, Canada, for their great support.

References

- [1] Avery T. Self-compacting concrete powerful tool for complicated pours. *Concr Monthly – News Cem Concr Industries* 2004;2(3).
- [2] Bouzoubaâ N, Lachemi M. Self-compacting concrete incorporating high volumes of class F fly ash: preliminary results. *Cem Concr Res* 2001;31(3):413–20.
- [3] Lachemi M, Hossain KMA, Lambros V, Bouzoubaâ N. Development of cost-effective self-compacting concrete incorporating fly ash, slag cement or viscosity modifying admixtures. *ACI Mater J* 2003;100(5):419–25.
- [4] Lachemi M, Hossain KMA, Lambros V, Nkinamubanzi PC, Bouzoubaâ N. Self-compacting concrete incorporating new viscosity modifying admixtures. *Cem Concr Res* 2004;24(6):917–26.
- [5] Patel R, Hossain KMA, Shehata M, Lachemi M. Development of statistical models for the mix design of high volume fly ash self-compacting concrete. *ACI Mater J* 2004;101(4):294–302.
- [6] Khayat KH, Paultre P, Tremblay S. Structural performance and in-place properties of self-consolidating concrete used for casting highly reinforced columns. *ACI Mater J* 2001;98(5):371–8.
- [7] Domone PL. A review of the hardened mechanical properties of self-compacting concrete. *Cem Concr Comp* 2007(29):1–12.
- [8] Lachemi M, Hossain KMA, Lambros V. Shear resistance of self-consolidating concrete beams – experimental investigations. *Can J Civil Eng* 2005;32(6):1103–13.
- [9] Taylor HPJ. The fundamental behavior of reinforced concrete beams in bending and shear. *ACI SP-42*, Detroit 1974:43–77.
- [10] Collins MP, Mitchell D, Adebar A, Vecchio FJA. General shear design method. *ACI Struct J* 1996;93(1):36–45.
- [11] Bazant ZP, Kim JK. Size effect in shear failure of longitudinally reinforced beams. *ACI J* 1984;81:456–68.
- [12] Bazant ZP, Kazemi MI. Size effect on diagonal shear failure of beams without stirrups. *ACI J* 1991;88:268–76.
- [13] Walraven J, Lehwalter N. Size effects in short beams loaded in shear. *ACI Struct J* 1994;91(5):585–93.
- [14] Bentz EC. Empirical modeling of reinforced concrete shear strength size effect for members without stirrups. *ACI Struct J* 2005;102:232–41.
- [15] Tompos EJ, Frosch RJ. Influence of beam size, longitudinal reinforcement, and stirrup effectiveness on concrete shear strength. *ACI J* 2002;99(5):559–67.
- [16] Zararis PD, Papadakis GC. Diagonal shear failure and size effect in RC beams without web reinforcement. *ASCE J Struct Div* 2001;127(7):733–41.
- [17] Kani GNJ. Basic facts concerning shear failure. *ACI J* 1966;63:675–92.
- [18] Kani GNJ. How safe are our large reinforced concrete beams. *ACI J* 1967;64:128–41.
- [19] Kani GNJ, Huggins MW, Wittkopp RR. Shear in reinforced concrete. Toronto: University of Toronto Press; 1979. p. 225.
- [20] ASTM C 494-99a. Standard specification for chemical admixtures for concrete. American Society for Testing and Materials, 2001.
- [21] ASTM C 143. Standard test method for slump of hydraulic-cement concrete. American Society for Testing and Materials, 2001.
- [22] Nagataki S, Fujiwara H. Self-compacting property of highly flowable concrete. *ACI SP 154*, Las Vegas, USA, 1995, p. 301–14.
- [23] Ozawa K, Sakata N, Iwai M. Evaluation of self-compactibility of fresh concrete using funnel test. *Proc. JSCE* 1994;23:490.
- [24] Sonebi M, Batros P, Zhu W, Gibbs J, Tamimi A. Properties of hardened concrete, Task 4, final report. Advance concrete masonry center, University of Paisley, Scotland, UK, 2000, p. 6–73.
- [25] ASTM C 39. Standard test method for compressive strength of cylindrical concrete specimens. American Society for Testing and Materials, 2001.
- [26] ASTM C 496-96. Standard test method for splitting tensile strength of cylindrical concrete specimens. American Society for Testing and Materials, 2001.
- [27] Lessard M, Talbot C, Phelan WS, Baker D. Self-consolidating concrete solves challenging placement problems at the Pearson International Airport in Toronto, Canada. In: 1st North American conference on the design and use of self-consolidating concrete (SCC), Rosemont, Illinois, 2002, p. 12–3.
- [28] MacGregor J, Barlett F. Reinforced concrete, mechanisms and design. 1st Canadian ed. Toronto, Canada: Prentice hall; 2000. p. 1042.
- [29] ACI Committee 318, 2005. Building code requirements for structural concrete (ACI 318-05) and commentary (ACI 318R-05). American Concrete Institute, Farmington Hills, Michigan, p. 151.
- [30] CSA CAN3-A23.3, 2004. Design of concrete structures. Canadian Standards Association, Rexdale, Ontario.
- [31] Collins MP, Kuchma D. How safe are our large, lightly reinforced concrete beams, slabs, and footings? *ACI Struct J* 1999;96(4):482–90.